Transport in Porous Media **26:** 229–260, 1997.

© 1997 *Kluwer Academic Publishers. Printed in the Netherlands.*

Effective Relative Permeabilities and Capillary Pressure for One-Dimensional Heterogeneous Media

MAGNAR DALE[1], STEINAR EKRANN[2], JOHANNES MYKKELTVEIT[2] and GEORGE VIRNOVSKY[2]
[1]*Rogaland University Center, Stavanger, Norway; e-mail: magnar.dale@tn.his.no*
[2]*RF – Rogaland Research, Stavanger, Norway*

(Received: 29 November 1995; in final form: 22 November 1996)

Abstract. The paper presents an analytical construction of effective two-phase parameters for one-dimensional heterogeneous porous media, and studies their properties. We base the computation of effective parameters on analytical solutions for steady-state saturation distributions. Special care has to be taken with respect to saturation and pressure discontinuities at the interface between different rocks. The ensuing effective relative permeabilities and effective capillary pressure will be functions of rate, flow direction, fluid viscosities, and spatial scale of the heterogeneities.

The applicability of the effective parameters in dynamic displacement situations is studied by comparing fine-gridded simulations in heterogeneous media with simulations in their homogeneous (effective) counterparts. Performance is quite satisfactory, even with strong fronts present. Also, we report computations studying the applicability of capillary limit parameters outside the strict limit.

Key words: heterogeneous porous media, effective relative permeabilities, effective capillary pressure.

Nomenclature

C	the interval $[p_c^{\min}, p_c^{\max}]$,
$\Delta_{i,j}(S)$	saturation discontinuity function, Equations (16) and (17),
ε	capillary number, Equation (59),
f	fractional flow of water,
$F(S)$	function defined in Equation (51),
ϕ	porosity,
$\Phi(S)$	function defined in Equation (5),
γ	interfacial tension,
I	$[S_{wc}, 1 - S_{or}]$,
$J(S)$	Leverett J-function,
k	absolute permeability,
k_H	harmonic mean of absolute permeability,
$k_{rj}(S)$	phase j relative permeability,
l	length of homogeneous rock,
L	length of period, Σl_i,
μ_j	phase j viscosity,
M	viscosity ratio μ_w/μ_o,
N	number of rocks in one period,
N_e	dimensionless number, Equation (48),
$p_c(S)$	capillary pressure function,

$\tilde{p}_c$	capillary pressure value,
P_c	capillary pressure reference value,
$p_c^{\max}$	$\min_i\{p_c^i(S_{wc}^i)\}$,
$p_c^{\min}$	$\max_i\{p_c^i(1-S_{or}^i)\}$,
$(\Delta p_c)_i$	capillary pressure discontinuity, Equation (30),
$p_j(x)$	phase j pressure,
Δp_j	phase j total pressure drop,
$(\Delta p_j)_i$	phase j pressure drop over ith rock,
$\Psi(S)$	function defined in Equation (6),
u_j	phase j Darcy velocity,
S	water saturation,
S_{wc}	irreducible water saturation,
S_{or}	residual oil saturation,
S_a	asymptotic saturation, Equation (7),
$S(u, S_N)$	saturation profile determined by $S_N \in I_N$ and $u \geqslant 0$,
$S_{u,f}$	the periodic saturation profile, $f \in [0,1]$, $u \geqslant 0$,
(S_i)	piecewise constant saturation profile,
$S(x_i^+)$	right-hand saturation at x_i,
$S(x_i^-)$	left-hand saturation at x_i,
u	total Darcy velocity,
x	spatial coordinate,
x_i	boundary, rocks i and $i+1$,

Subscripts/Superscripts

i	refers to ith rock,
j	oil (o) or water (w) phase,
$\langle - \rangle$	spatial averaging,
cap	effective, at capillary limit,
eff	effective,
visc	effective, at viscous limit,

1. Introduction

Upscaling of flow parameters from core scale to numerical gridblock scale is a problem of practical importance. If the classical separation of scales condition is satisfied, see Section 2, *effective parameters*, do this job. Effective parameters depend only on physical properties of the flow system, and appear as coefficients in the differential equations for large scale variables. The relation to the complementary concept of *dynamic pseudo functions*, is discussed in Ekrann and Dale, [11].

In this paper we solve the effective parameter problem for one-dimensional media. The one-dimensional geometry is sometimes of direct relevance, such as to composite cores or to vertical flow in layered reservoirs. More importantly, the completeness of the solution obtained provides a firm basis for generalizations into higher dimensions.

In general, the difficult part of the problem is to determine the small scale saturation distributions. Once these are established, one may in principle obtain

the two-phase effective parameters by applying some one-phase method for each distribution. Most authors have imposed the condition of *capillary equilibrium*, implying that local saturation is determined exclusively by the local capillary pressure curve. By restricting our study to one-dimensional, an analytical approach is possible, whereby we are able to extend the existing results to saturation distributions determined by a balance between viscous and capillary forces.

Assuming a spatially periodic heterogeneous medium, the separation of scales condition requires periodic saturation and pressure gradient profiles, hence the heterogeneity period (unit cell) can be used as the averaging volume. The assumption of periodicity is not as restrictive as it may seem. In principle, random heterogeneities can be handled by making the period sufficiently large.

Our approach makes it possible to study analytically the rate dependence of effective parameters. As the rate tends to zero, capillary equilibrium effective parameters are recovered. Similarly, as the rate tends to infinity, viscous limit effective parameters are approached. As a particular case of rate dependence, we also discuss dependence on flow direction.

We impose no special conditions on the different relative permeability and capillary pressure curves associated with the different rocks making up the heterogeneous medium. Different capillary pressure curves are allowed to take different values in their endpoint saturations. Phase pressures will not necessarily be continuous at boundaries between different rocks, hence effective relative permeabilities are not always obtained simply by harmonic averaging of phase permeabilities along the saturation profiles. As another consequence, capillary trapping may occur.

The applicability of effective parameters in dynamic displacement situations is demonstrated by comparing fine-gridded simulations in the original heterogeneous media with simulations in their homogeneous (effective) counterparts. Performance is quite satisfactory, even with strong fronts present, thus violating the separation of scales condition. Generally, the condition is thought to be overly severe (Quintard and Whitaker [19]).

Capillary limit effective parameters are the easiest to compute, in particular in higher dimensions. A question of practical interest, therefore, is to what extent and under what circumstances capillary limit results are applicable outside the strict limit. A set of experiments is reported and analyzed, indicating that capillary limit effective parameters can be guaranteed to be accurate only for sub meter-scale heterogeneities.

2. Separation of Scales

Consider two-phase flow in a heterogeneous porous medium. Let l_k denote the spatial scale of rock heterogeneities; similarly, l_S and l_p denote the spatial scales for small-scale variation of saturation and pressure gradients, respectively. Let large scale quantities be defined via spatial averaging, with L being the averaging scale, and denote by $\mathcal{L}_k$, $\mathcal{L}_S$ and $\mathcal{L}_p$ the spatial scales over which averaged rock properties,

averaged saturation and averaged pressure gradients change significantly. Then the *separation of scales* condition can be summarized as

$$l_k, l_S, l_p \ll L \ll \mathcal{L}_k, \mathcal{L}_S, \mathcal{L}_p. \tag{1}$$

In particular, the condition implies that large-scale quantities must be approximately constant on the scale L of averaging. Note that the condition includes both rock properties and flow variables.

We also need to assume that boundaries do not influence the small-scale behaviour of flow. In other words, for a given large-scale pressure gradient and large-scale saturation, the small-scale pressure and saturation distribution should be completely determined by the medium itself, and possibly, by the local value of large-scale velocities. In addition, one must require history to be forgotten, in the sense that the small-scale saturation distribution must have had time to obtain a final shape (developed flow). As formulated, these conditions are rather qualitative, as is the separation of scales condition. This reflects the fact that formulation in terms of effective properties can only be approximate (Ekrann [13]).

When the conditions are satisfied, one can show that the large-scale variables satisfy equations of the same form as the local Darcy equations, with effective absolute and relative permeabilities and capillary pressure replacing their local counterparts (Quintard and Whitaker [17, 18]).

3. Steady Two-Phase Flow in a Heterogeneous Medium

3.1. STEADY FLOW IN A HOMOGENEOUS MEDIUM

3.1.1. *Equations*

We consider steady-state, incompressible, immiscible flow of oil and water in a homogeneous one-dimensional porous medium. Neglecting gravity effects, the Darcy equations and capillary pressure relation in conventional notation read

$$u_j = -\frac{k k_{rj}(S(x))}{\mu_j} \frac{\mathrm{d}p_j}{\mathrm{d}x}(x), \tag{2}$$

$$p_c(S(x)) = p_o(x) - p_w(x), \tag{3}$$

where S is water saturation and $j = o, w$ is the fluid phase.

We shall assume throughout that individual phase velocities $u_w, u_o \geqslant 0$. Mass conservation dictates u_o and u_w to be constant, as well as the total Darcy velocity, $u = u_w + u_o$, and the fractional flow of water, $f = u_w/u \in [0, 1]$. Assuming $u > 0$, the following expression for f is easily derived (see Marle [15], Chapter 14)

$$f = \Phi(S) + \Psi(S)\frac{\mathrm{d}S}{\mathrm{d}x}, \tag{4}$$

where

$$\Phi(S) = \frac{\mu_o k_{rw}}{\mu_o k_{rw} + \mu_w k_{ro}}, \tag{5}$$

$$\Psi(S) = \frac{k}{u} \frac{k_{rw} k_{ro}}{\mu_o k_{rw} + \mu_w k_{ro}} \frac{\mathrm{d}p_c}{\mathrm{d}S}. \tag{6}$$

Here S varies in the closed saturation interval $I = [S_{wc}, 1 - S_{or}]$. We assume that $k_{rw}(S_{wc}) = k_{ro}(1 - S_{or}) = 0$, with k_{rw} strictly increasing on I, k_{ro} strictly decreasing. The capillary pressure curve $p_c(S)$ may have a finite value or a vertical asymptote at the endpoints of I. In the interior of I we assume $\mathrm{d}p_c/\mathrm{d}S < 0$, possibly with $\mathrm{d}p_c/\mathrm{d}S = -\infty$ at one or both endpoints. Thus $\Psi < 0$ in the interior of I. At an endpoint of I either $\Psi = 0$ or Ψ tends to $-\infty$.

The function Φ is differentiable and strictly increasing from $0 = \Phi(S_{wc})$ to $1 = \Phi(1 - S_{or})$. For each $f \in [0, 1]$ denote by $S_a = S_a(f)$ the *asymptotic saturation* corresponding to f, defined by

$$\Phi(S_a) = f. \tag{7}$$

3.1.2. *Saturation Profiles*

Let l denote the length of the medium, so that $x \in [0, l]$. Each *outlet* saturation boundary condition

$$S(l) = S_1 \in I \tag{8}$$

uniquely determines a solution $S(x)$ of Equation (4). To see this, first let $u = 0$; then obviously the solution is the constant $S(x) = S_1$ for each $S_1 \in I$. Thus, for the rest of the discussion we may assume $u > 0$; write the equation in the form

$$\frac{\mathrm{d}S}{\mathrm{d}x} = H(S) = \frac{f - \Phi(S)}{\Psi(S)}. \tag{9}$$

In general, the behaviour of the solutions is determined by the zeros of H. First assume that $f \neq 0, 1$. Then S_a is the only zero of H in the interior of I; hence $S_1 = S_a$ determines the constant solution $S(x) = S_a$. For $S_1 \neq S_a, S_{wc}, 1 - S_{or}$, the inverse of the solution determined by S_1 is obtained by integration

$$x(S) = l + \int_{S_1}^{S} \frac{\Psi}{f - \Phi} \, \mathrm{d}\tilde{S}. \tag{10}$$

Considering the sign of the integrand, it is clear that $S(x)$ is strictly decreasing if $S_{wc} < S_1 < S_a$, strictly increasing if $1 - S_{or} > S_1 > S_a$. The integral diverges as

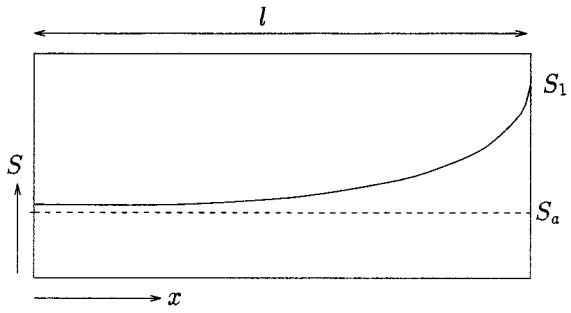

Figure 1. Saturation approach to asymptotic.

S tends to S_a; hence, the line $S = S_a$ acts as an asymptote for the solution. It is approached by $S(x)$ in the negative x-direction from above or below according to whether $S_1 > S_a$ or $S_1 < S_a$, see Figure 1.

At an endpoint $S_e \in \{S_{wc}, 1 - S_{or}\}$ of I we distinguish two cases. First, if $\Psi \to -\infty$ as $S \to S_e$, we set $H(S_e) = 0$; thus, $S_1 = S_e$ determines the constant solution $S(x) = S_e$. (Obviously, this case is not physically meaningful, since only one mobile phase is present, while $f \neq 0, 1$, i.e. two phases are flowing.) On the other hand, if $\Psi \to 0$ as $S \to S_e$, the solution is again determined by (10). Note that in this case $|\mathrm{d}S/\mathrm{d}x| \to \infty$ as $x \to l$.

Now assume $f = 0$ (the case $f = 1$ is analogous). First, for $S_1 = S_{wc} = S_a$ we have $S(x) = S_{wc}$, the limiting solution as $f \to 0$. For $S > S_{wc}$ we get

$$\frac{\mathrm{d}S}{\mathrm{d}x} = H(S) = -\frac{u\mu_o}{kk_{ro}\,\mathrm{d}p_c/\mathrm{d}S}. \tag{11}$$

If $k_{ro}\,\mathrm{d}p_c/\mathrm{d}S \to -\infty$ at $1 - S_{or}$, the condition $S_1 = 1 - S_{or}$ determines the constant solution $S(x) = 1 - S_{or}$, or else we have $k_{ro}\,\mathrm{d}p_c/\mathrm{d}S = 0$ at $1 - S_{or}$, and the solution is obtained by integration

$$x(S) = l - \frac{k}{u\mu_o}\int_{S_1}^{S} k_{ro}(\mathrm{d}p_c/\mathrm{d}\tilde{S})\,\mathrm{d}\tilde{S}, \tag{12}$$

valid for $S_{wc} < S_1 \leqslant 1 - S_{or}$, $S \leqslant S_1$. If $0 < x(S_{wc}) < \infty$, then the solution $S(x)$ determined by (12) is defined only for $x \in [x(S_{wc}), l]$; in this case we extend to a continuous solution on $[0, l]$ by setting $S(x) = S_{wc}$ for $x \in [0, x(S_{wc})]$.

Finally, note that there may be no solution to Equation (4) satisfying the *inlet* boundary condition $S(0) = S_1$. In general, the integral in (10) tends to a finite value as S tends to the endpoint saturations S_{wc} or $1 - S_{or}$. If l is sufficiently large, $S(x)$ will have reached one of the end-point saturations for $x < l$, at which point the solution breaks down. Consequently, in discussing the heterogeneous case later, we shall always assume the boundary condition to be given at the outlet, and construct the solution from right to left.

3.1.3. *Pressure Drops*

Any saturation solution $S(x)$ satisfying $S_{wc} < S(x) < 1 - S_{or}$ uniquely determines the phase pressure profiles $p_j(x)$ by specifying a pressure boundary condition for one of the phases and integrating Equation (2). In particular, the corresponding phase pressure drops $\Delta p_j = p_j(0) - p_j(l)$ are given by the expression

$$\Delta p_j = \frac{u_j \mu_j}{k} \int_0^l \frac{1}{k_{rj}(S(x))} \, \mathrm{d}x. \tag{13}$$

However, if $S(x) = S_e \in \{S_{wc}, 1 - S_{or}\}$ for some $x \in [0, l]$, one of the phase pressures will become infinite, unless p_c is finite at the endpoint S_e. In this case, if $S(x) < 1 - S_{or}$, but $S(x) = S_{wc}$ for some x, then Δp_o is again given by (13), and we may determine Δp_w from the relation

$$\Delta p_w = \Delta p_o - p_c(S(0)) + p_c(S(l)). \tag{14}$$

The situation is analogous if $S(x) > S_{wc}$, and $S(x) = 1 - S_{or}$ for some x.

Finally, for $f = 0$ the saturation profile determined by $S_1 = S(l) = 1 - S_{or}$ might also reach $S(x) = S_{wc}$. In this case we first determine $p_w(x)$ in some neighbourhood of l, and define $p_o(x) = p_w(x) + p_c(S(x))$ here; next extend $p_o(x)$ continuously to all of $[0, l]$, and use it to define $p_w(x) = p_o(x) - p_c(S(x))$. – The discussion is analogous for $f = 1$.

3.2. STEADY FLOW IN A HETEROGENEOUS MEDIUM

3.2.1. *Description of Medium*

We consider a semi-infinite periodic one-dimensional porous medium $(-\infty, L]$ with period $[0, L]$, see Figure 2. The N rocks constituting the period are defined by their length, l, and properties, ϕ, k, k_{rw}, k_{ro} and p_c. Neighbouring rocks differ in at least one of their rock properties. The rocks are numbered from left to right. Rock boundaries are positioned at $0 = x_0 < x_1 < \cdots < x_N = L$, so that $x_i - x_{i-1} = l_i$ is the length of the ith rock.

3.2.2. *The Saturation Discontinuity Function*

Consider the N capillary pressure functions $p_c^i(S)$, $S \in I_i = [S_{wc}^i, 1 - S_{or}^i]$ (where possibly p_c tends to $-\infty$ at the right endpoint of I, and to ∞ at the left one). For each ordered pair of integers (i, j), $i, j = 1, \ldots, N$, we define a function

$$\Delta_{i,j} \colon I_i \to I_j, \tag{15}$$

associating saturations in I_i and I_j having the same capillary pressure. Thus we set

$$\Delta_{i,j}(S) = (p_c^j)^{-1}(p_c^i(S)), \tag{16}$$

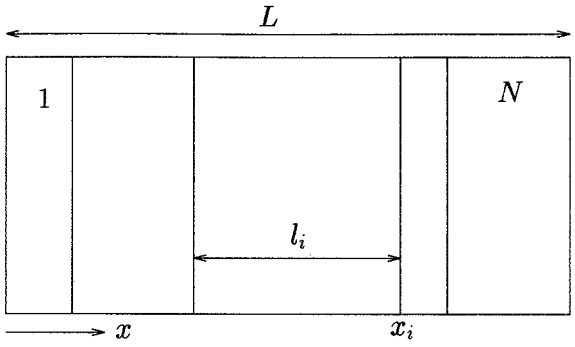

Figure 2. Period of a periodic medium.

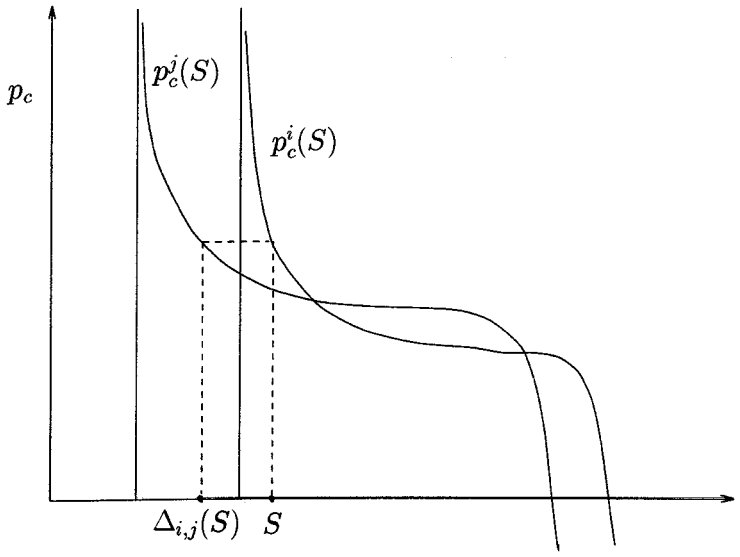

Figure 3. The saturation discontinuity function.

see Figure 3.

However, this function is well defined only if the range of p_c^i is contained in the range of p_c^j. If this is not the case, we extend $\Delta_{i,j}$ to all of I_i simply by setting

$$\Delta_{i,j}(S) = \begin{cases} S_{wc}^j & \text{if } p_c^i(S) > p_c^j(S_{wc}^j), \\ 1 - S_{or}^j & \text{if } p_c^i(S) < p_c^j(1 - S_{or}^j). \end{cases} \tag{17}$$

If p_c^i and p_c^j have the same range, $\Delta_{i,j}$ and $\Delta_{j,i}$ are both monotonically increasing, with $(\Delta_{i,j})^{-1} = \Delta_{j,i}$. In particular, $\Delta_{i,j}$ maps the endpoint saturations of I_i to those of I_j.

3.2.3. *Interface Conditions*

Fix a fractional flow $f \in [0,1]$, and assume first a total velocity $u > 0$. A saturation profile $S(x)$ in the period $[0, L]$ will be called *steady state* if it satisfies Equation (4) in each rock, and

$$\Delta_{i+1,i}(S(x_i^+)) = S(x_i^-) \tag{18}$$

at each boundary x_i between rocks. Superscripts $+$ and $-$ indicate limiting values as x_i is approached from above and below, respectively. For $i = 0$ we set

$$S(x_0^-) = \Delta_{1,N}(S(x_0^+)). \tag{19}$$

If $u = 0$, the saturation is constant S_i in each rock i, as discussed previously, and we require

$$\Delta_{i+1,i}(S_{i+1}) = S_i. \tag{20}$$

The pressure profiles $p_w(x)$ and $p_o(x)$ corresponding to a steady state saturation profile $S(x)$ must satisfy the capillary condition in each rock $x \in (x_{i-1}, x_i)$

$$p_o(x) - p_w(x) = p_c^i(S(x)). \tag{21}$$

Note that the imposed conditions (18) and (20) may lead to discontinuous capillary pressure at some of the boundaries, in which case one of the individual phase pressures also needs to be discontinuous. This happens only if the water saturation or the oil saturation becomes irreducible at x_i^-, as can be seen from Definition (17). In this case, if $S(x_i^-) = S_{wc}^i$ we require the oil pressure p_o to be continuous at x_i and determine the discontinuity of the water pressure p_w by setting

$$p_w(x_i^-) = p_o(x_i) - p_c^i(S_{wc}^i). \tag{22}$$

Similarly, if $S(x_i^-) = 1 - S_{or}^i$ we require continuity of water pressure at x_i and determine the oil pressure discontinuity by

$$p_o(x_i^-) = p_c^i(1 - S_{or}^i) + p_w(x_i). \tag{23}$$

Note that in (22), (23) the capillary pressure at the endpoints of I is finite, by definition of the Δ – function.

For a proof that this treatment of pressure discontinuities is correct, see van Duijn *et al.* [9] or Dale [8].

3.2.4. *Solution of Saturation Boundary-Value Problem*

Fix a value of the fractional flow $f \in [0,1]$. For any $u \geqslant 0$ and outlet saturation $S_N \in I_N$ there is a unique steady state saturation profile $S(x)$, denoted by

$S(u, S_N)(x)$, satisfying the outlet boundary condition $S(x_N^-) = S_N$: Over the Nth rock the solution is uniquely determined by the results of Section 3.1. Hence, by (18) a boundary condition at the outlet of rock $N-1$ is established, and the solution over $[0, L]$ can be completed recursively.

The steady state piecewise constant profiles $S(0, S_N)(x)$ denoted by $S_i, x \in (x_{i-1}, x_i)$, will be called *capillary equilibrium*, profiles, see Section 4.3 below.

3.2.5. *Periodic Solutions*

A steady state saturation profile $S(x)$ is *periodic* over $[0, L]$ if

$$S(x_0^-) = S(x_N^-). \tag{24}$$

To prove the existence of a periodic steady-state solution for each $f \in [0, 1]$, consider the map $I_N \to I_N$ defined by

$$S_N \mapsto S(u, S_N)(x_0^-). \tag{25}$$

The steady-state solution $S(u, S_N)$ is periodic if and only if S_N is a fixpoint for this map, by Definition 24. Thus, it suffices to check continuity of the map, since I_N is a closed interval. But this is clear, since the function defined by (25) is a composition of continuous functions, namely the Δ-functions and the functions $S(u, S_N)(x_i^-) \mapsto S(u, S_N)(x_{i-1}^+)$ associating the inlet saturation to the outlet saturation in each rock.

Under mild conditions on the behaviour of relative permeability and capillary pressure at the endpoints of I, a periodic solution is unique, see Dale [8].

3.2.6. *Total Pressure Drops*

For any steady-state sauration profile $S(x)$, the corresponding phase j total pressure drops

$$\Delta p_j = p_j(x_0^-) - p_j(x_N^-) \tag{26}$$

are given by

$$\Delta p_w = \sum_{i=1}^{N} (\Delta p_w)_i + \sum_{i \in A_w} (\Delta p_c)_i, \tag{27}$$

$$\Delta p_o = \sum_{i=1}^{N} (\Delta p_o)_i + \sum_{i \in A_o} (-\Delta p_c)_i. \tag{28}$$

Here, A_j denotes the set of boundary indices i, $0 \leqslant i \leqslant N-1$, where phase j pressure is discontinuous. Further, $(\Delta p_j)_i$ is the phase j pressure drop over the ith rock

$$(\Delta p_j)_i = p_j(x_{i-1}^+) - p_j(x_i^-) \tag{29}$$

discussed previously. Finally,

$$(\Delta p_c)_i = p_c^{i+1}(S(x_i^+)) - p_c^i(S(x_i^-)) \tag{30}$$

is the capillary pressure jump across boundary x_i. Note that $(\Delta p_c)_i < 0$ when $i \in A_o$. In particular, if $S(x)$ is a saturation profile along which the capillary pressure is continuous, the right-hand sides of (27) and (28) reduce to the sum of pressure drops over the individual rocks.

Note that the water and oil total pressure drops corresponding to a periodic saturation solution are equal

$$\Delta p_w = \Delta p_o. \tag{31}$$

This follows immediately from the definitions.

4. Effective Parameters

4.1. THE GENERAL CASE

Consider a steady state saturation profile and the corresponding pressure profiles in a periodic medium. If the saturation is periodic, obviously the saturation averaged over the full period is constant throughout the medium. Also, the averaged pressure gradients are constant. Hence, the small and large scales are separated using the heterogeneity period as the averaging scale. The effective relative permeability functions, k_{rw}^{eff} and k_{ro}^{eff}, and the effective capillary pressure, p_c^{eff}, are then coefficients in equations of the same form as the local Darcy equations. More precisely, for any fractional flow $f \in [0, 1]$ and total velocity $u \geqslant 0$, let $S(x)$, $p_w(x)$, $p_o(x)$ be the corresponding periodic steady state saturation and pressure profiles. Let $S_{\text{eff}} = S_{\text{eff}}(f)$ denote the average saturation in the period,

$$S_{\text{eff}} = \frac{\langle \phi(x) S(x) \rangle}{\langle \phi(x) \rangle}. \tag{32}$$

Then

$$u_j = \frac{k_H k_{rj}^{\text{eff}}(S_{\text{eff}})}{\mu_j} \frac{\mathrm{d}}{\mathrm{d}x} \langle p_j(x) \rangle, \tag{33}$$

$$p_c^{\text{eff}}(S_{\text{eff}}) = \langle p_o(x) \rangle - \langle p_w(x) \rangle, \tag{34}$$

where k_H is the harmonic mean, and $\langle\ \rangle$ denotes spatial averaging over the full period.

Obviously, Equation (34) is equivalent to

$$p_c^{\text{eff}}(S_{\text{eff}}) = \langle p_c(S(x)) \rangle. \tag{35}$$

Furthermore, $d\langle p_j(x)\rangle/\mathrm{d}x = \Delta p_j/L$. If $u > 0$, we have $\Delta p_w = \Delta p_o > 0$, thus Equation (33) can be inverted to yield

$$k_{rj}^{\text{eff}}(S_{\text{eff}}) = \frac{u_j \mu_j L}{k_H \Delta p_j}. \tag{36}$$

The effective irreducible water saturation is determined from the periodic saturation profile corresponding to $f = 0$: $S_{wc}^{\text{eff}} = S_{\text{eff}}(0)$. Similarly, $1 - S_{or}^{\text{eff}}$ results from $f = 1$. Thus, (35) and (36) uniquely determine the effective parameters on the effective saturation interval

$$I_{\text{eff}} = [S_{wc}^{\text{eff}}, 1 - S_{or}^{\text{eff}}] \tag{37}$$

by continuously varying $f \in [0, 1]$.

Define the effective fractional flow function Φ_{eff} by

$$\Phi_{\text{eff}} = \frac{\mu_o k_{rw}^{\text{eff}}}{\mu_o k_{rw}^{\text{eff}} + \mu_w k_{ro}^{\text{eff}}}. \tag{38}$$

For any $f \in [0, 1]$ it holds that

$$\Phi_{\text{eff}}(S_{\text{eff}}(f)) = f. \tag{39}$$

This follows immediately from Equation (36), since $\Delta p_w = \Delta p_o$ for a periodic solution.

Remark. The above construction produces well defined effective parameters for any heterogeneous medium where Ψ tends to zero at the endpoints of I, in each homogeneous rock (equivalently, $k_{rw}\,\mathrm{d}p_c\,\mathrm{d}S \to 0$ at S_{wc} and $k_{ro}\,\mathrm{d}p_c/\mathrm{d}S \to 0$ at $1 - S_{or}$). This condition will guarantee that (if $f \neq 0, 1$) a steady state profile may attain one of the end point values $S_{wc}, 1 - S_{or}$ of I only at an *outlet* x_i^- of a homogeneous rock. Conversely, allowing $\Psi \to -\infty$ at one or both endpoints of I, there exist media where, for fixed $f \neq 0, 1$, the (unique) periodic saturation profile is physically meaningless.

4.2. SPECIAL CASE

Assume that all capillary pressure curves have the same range. In this case there are no pressure discontinuities, and effective relative permeabilities are given by harmonic averaging, see Equations (13) and (36)

$$k_{rj}^{\text{eff}}(S_{\text{eff}}) = \frac{L}{k_H} \left(\int_0^L \frac{1}{k(x) k_{rj}(S(x))}\,\mathrm{d}x \right)^{-1}. \tag{40}$$

4.3. CAPILLARY LIMIT EFFECTIVE PARAMETERS

In the limit of zero total velocity the steady state saturation profiles are the locally constant capillary equilibrium profiles $S(0, S_N)$. However, the total phase pressure drops will also be zero, hence effective relative permeabilities are not determined by Equation (36) in this case. Therefore it is necessary to define separately the *capillary limit* effective parameters.

We first determine the periodic capillary equilibrium saturation profiles. Define

$$p_c^{\min} = \max_i \{p_c^i(1 - S_{or}^i)\}, \qquad p_c^{\max} = \min_i \{p_c^i(S_{wc}^i)\}. \tag{41}$$

First assume $p_c^{\min} \leqslant p_c^{\max}$, so that the interval $C = [p_c^{\min}, p_c^{\max}]$ is the intersection of the ranges of the capillary pressure curves. In this case each capillary equilibrium profile (S_i) is uniquely determined by choosing a capillary pressure value $\tilde{p}_c \in C$, and put

$$S_i = (p_c^i)^{-1}(\tilde{p}_c). \tag{42}$$

As $\tilde{p}_c$ varies continuously in C let S_{eff} denote the effective saturation of the corresponding equilibrium profile.

Now define the capillary limit effective relative permeabilities by harmonic averaging

$$k_{rj}^{\text{cap}}(S_{\text{eff}}) = \frac{L}{k_H} \left(\sum_{i=1}^{N} \frac{l_i}{k_i k_{rj}^i(S_i)} \right)^{-1} \tag{43}$$

and define capillary limit effective capillary pressure by

$$p_c^{\text{cap}}(S_{\text{eff}}) = \tilde{p}_c. \tag{44}$$

In the profile corresponding to $\tilde{p}_c = p_c^{\min}$, respectively $\tilde{p}_c = p_c^{\max}$, we have $S_i = 1 - S_{or}^i$, respectively $S_i = S_{wc}^i$, for at least one i. By Equation (43), the corresponding effective phase permeability then becomes zero, thus $p_c^{\max}$ and $p_c^{\min}$ give rise to the capillary limit endpoint saturations S_{wc}^{cap} and $1 - S_{or}^{\text{cap}}$. As $\tilde{p}_c$ varies continuously in C the effective saturation of the corresponding profile spans the capillary limit saturation interval, $I_{\text{cap}} = [S_{wc}^{\text{cap}}, 1 - S_{or}^{\text{cap}}]$. Note that the endpoint saturations are equal to the arithmetic average of their rock counterparts only if the capillary pressure curves all have the same range.

If $p_c^{\min} > p_c^{\max}$, the ranges of the capillary pressure curves have no point in common. Obviously, the capillary pressure along an equilibrium profile cannot be continuous in this case, hence the total pressure drops Δp_w and Δp_o are both nonzero. It follows from Equation (36) that the effective relative permeability curves are both identically zero.

One can prove that the capillary limit effective parameters defined by (43) and (44) are indeed the limits, as u tends to zero, of the effective parameters defined in Equations (35), (36) (Mykkeltveit [16]).

4.4. VISCOUS LIMIT EFFECTIVE PARAMETERS

As the total Darcy velocity u increases, viscous forces increase in importance. In the limit of infinite u, Ψ becomes zero. This is the viscous limit. According to Equation (4), the saturation in the ith rock is then constant. Thus, each $f \in [0,1]$ determines a piecewise constant saturation by

$$S_i = (\Phi_i)^{-1}(f). \tag{45}$$

Now define the viscous limit effective parameters by

$$k_{rj}^{\text{visc}}(S_{\text{eff}}) = \frac{L}{k_H}\left(\sum_{i=1}^{N}\frac{l_i}{k_i k_{rj}^i(S_i)}\right)^{-1}, \tag{46}$$

$$p_c^{\text{visc}}(S_{\text{eff}}) = \frac{1}{L}\sum_{i=1}^{N} l_i p_c^i(S_i), \tag{47}$$

where S_{eff} is the average saturation of the profile (S_i). Obviously, to $f = 0$ there corresponds the profile (S_{wc}^i), while to $f = 1$ there corrresponds $(1 - S_{or}^i)$. Thus, the viscous limit endpoint saturations S_{wc}^{visc} and $1 - S_{or}^{\text{visc}}$ are simply the weighted arithmetic average of their rock counterparts. As f varies continuously in $[0,1]$ the effective saturation of the corresponding profile spans the viscous limit effective saturation interval $I_{\text{visc}} = [S_{wc}^{\text{visc}}, 1 - S_{or}^{\text{visc}}]$.

The definitions of capillary limit and viscous limit effective parameters given above are very similar. The main difference occurs in the way the saturation distributions are computed. While piecewise constant in both cases, saturation distributions (42) and (45) may be fundamentally different, and may produce very different effective parameters.

The convergence of Equations (35), (36) towards viscous limit results (46), (47) as u tends to ∞ is proved in Dale [8].

5. Some Properties of Effective Parameters

5.1. RATE DEPENDENCE

As has been discussed in some detail, effective two-phase parameters should generally be expected to be rate-dependent. Equations (27) and (28) indicate that increasing the rate, keeping all other parameters fixed, will increase the relative importance of the viscous pressure drops Δp_j at the expense of the capillary discontinuities Δp_c, thereby altering effective relative permeabilities through Equation 36.

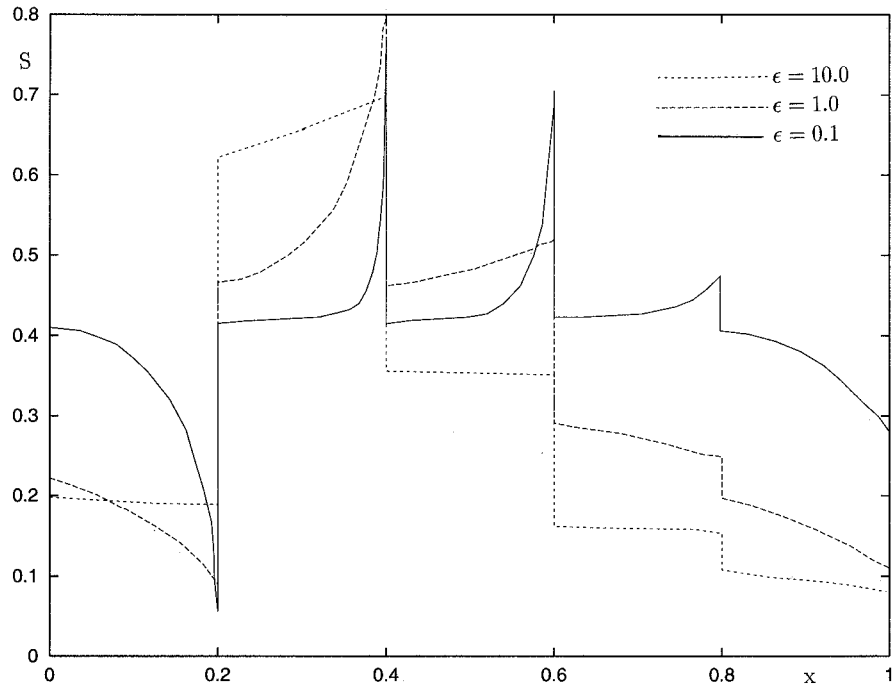

Figure 4. Saturation distributions in medium A, $f = 0.5$.

More subtly, the rate also influences the saturation distribution inside individual rocks, also in turn influencing effective capillary pressure and relative permeabilities. Figure 4 shows saturation distributions in medium A (nonlinear Leverett J-function) for three different values of the capillary number ε, which is inversely proportional to the rate (see Definition (59), Section 6). As can be seen, decreasing ε makes the saturation approach the asymptotic saturation more rapidly. The corresponding effective relative permeabilities are shown in Figure 5.

5.2. DIRECTIONAL DEPENDENCE

Effective parameters in general depend on direction of flow. An example is given in Figure 6, pertaining to medium B (nonlinear Leverett J-function), see Section 6. This directional dependence is brought about by directional dependence of the periodic saturation distribution, which will occur for $N \geqslant 3$. Note, however, that the capillary – and viscous limits effective parameters are independent of flow direction. This is a consequence of the piecewise constant saturation distributions in these cases, see Equations (42) and (45).

We would not expect directional dependence in an unordered (random) system. Some sort of systematic ordering (periodicity) would be required, as in the example shown.

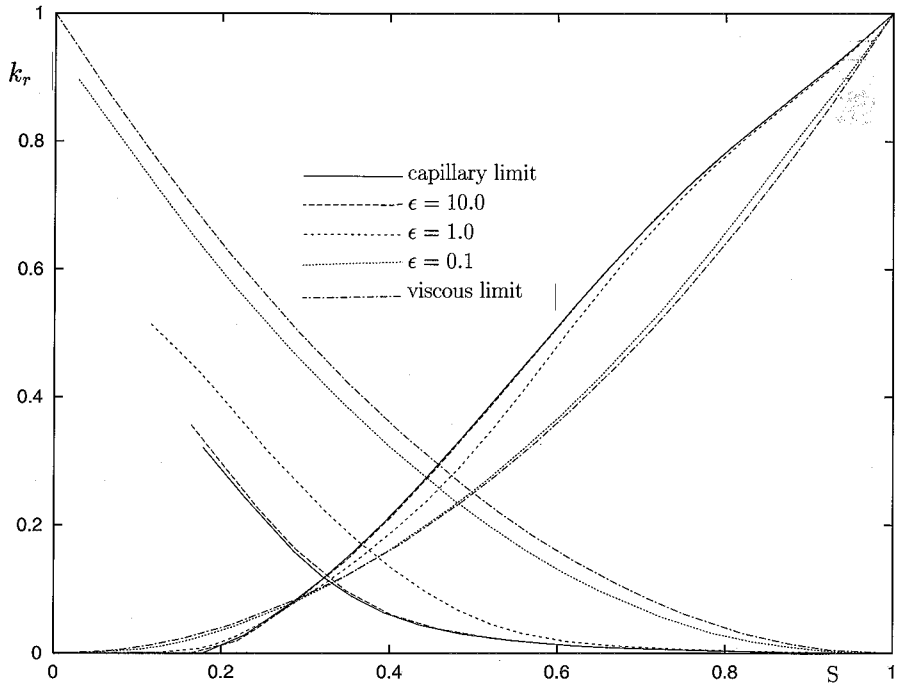

Figure 5. Effective relative permeabilities, medium A.

5.3. DEPENDENCE ON CORRELATION LENGTH

The effective properties depend on the absolute lengths of the homogeneous rocks in the period. More precisely, fixing the relative lengths of the homogeneous parts, the total length L acts as a correlation length for the heterogeneities. Furthermore, the effective parameters tend to the viscous limit parameters as L increases, since the periodic profile will tend to the constant asymptotic saturation in each homogeneous rock. Conversely, letting $L \to 0$ we obtain the capillary limit parameters.

5.4. SCALING PROPERTIES

Consider the class of media with a fixed number N of homogeneous rocks, where all the i-th rocks have the same relative length l_i/L, relative absolute permeability k_i/k_H, relative porosity ϕ_i/ϕ_A, relative capillary pressure curve p_c^i/P_c, and the same relative permeability curves. Here $\phi_A = \langle\phi(x)\rangle = (\Sigma\phi_i l_i)/L$ is the average porosity, and P_c is some capillary pressure representative value for the medium (for instance, the (absolute) average value of the p_c-curves at the midpoint of their saturation interval). We claim that *within this class of media, effective parameters depend only on the viscosity ratio $M = \mu_w/\mu_o$ and the dimensionless number*

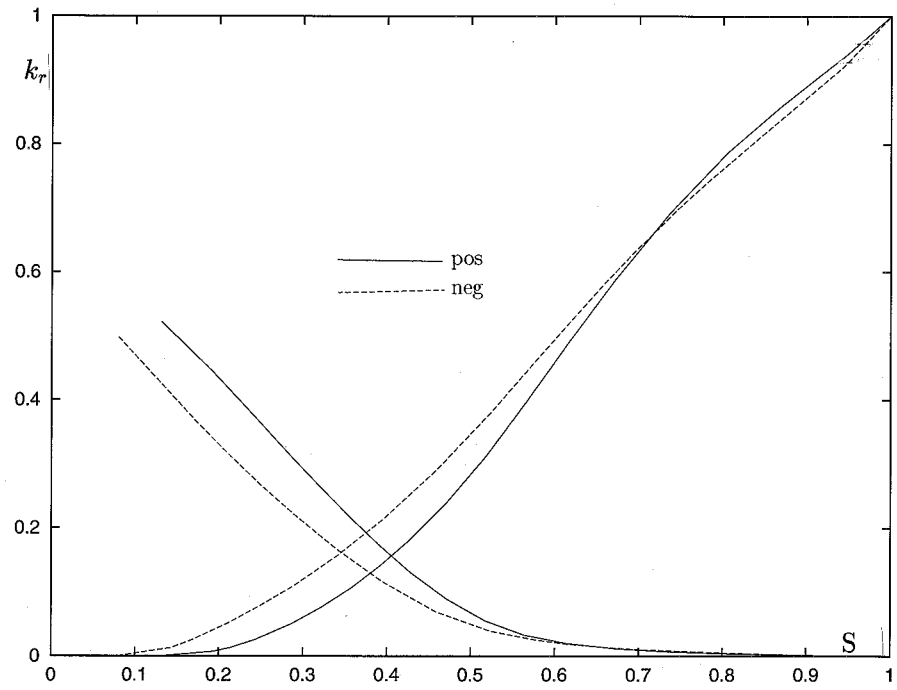

Figure 6. Effective relative permeabilities for medium B, $\varepsilon = 1$, positive and negative directions of flow.

$$N_e = \frac{Lu\mu_o}{k_H P_c}. \tag{48}$$

To show this, the crucial point is the following: Pick two media in the class, and choose flow parameters u, μ_w, μ_o for medium 1, u', μ'_w, μ'_o for medium 2. Fix a fractional flow f, and let $S(x), x \in [0, L]$, $S'(x), x \in [0, L']$ denote the corresponding periodic saturation profiles in the two media. We claim that if $M = M'$ and $N_e = N'_e$, then for all i, $i = 0, \ldots, N$

$$S_i^+ = S_i^{+'}, \qquad S_i^- = S_i^{-'}, \tag{49}$$

where we write $S_i^+ = S(x_i^+)$, etc.

In proving this, we consider $S(x)$ in medium 1 as given. Denote by $S_N = S(L^-)$ its left-hand outlet saturation; note that $S_0^- = S_N$, since $S(x)$ is assumed periodic. Now define $S'(x)$ to be the profile in medium 2 uniquely determined by the same outlet boundary condition as $S(x)$, i.e. $S'(L^{-'}) = S_N$. We will show that this profile has the properties (49); in particular, $S'(x)$ is the periodic profile in medium 2.

First recall that by Equation (10)

$$\int_{S_i^-}^{S_{i-1}^+} \frac{\Psi_i}{f - \Phi}\, \mathrm{d}S = l_i.$$

Note that the fractional flow function $\Phi(S)$ is the same for all rocks in both media. Thus, over rock N in medium 1 we have

$$\frac{u\mu_o}{k_N}\int_{S_N}^{S_{N-1}^+}\frac{\Psi_N}{f-\Phi}\,\mathrm{d}S=\frac{l_N u\mu_o}{k_N}=\int_{S_N}^{S_{N-1}^+}F_N(S)\,\mathrm{d}S, \tag{50}$$

where

$$F_i(S)=\frac{u\mu_o\Psi_i}{k_i(f-\Phi)}=\frac{k_{rw}k_{ro}dp_c^i/\mathrm{d}S}{(f-1)k_{rw}+Mfk_{ro}}. \tag{51}$$

Similarly, in medium 2

$$\frac{u'\mu_o'}{k_N'}\int_{S_N}^{S_{N-1}^{+'}}\frac{\Psi_N'}{f-\Phi}\,\mathrm{d}S=\frac{l_N'u'\mu_o'}{k_N'}=\frac{P_c'}{P_c}\int_{S_N}^{S_{N-1}^{+'}}F_N(S)\,\mathrm{d}S. \tag{52}$$

From our assumptions $l_i/L=l_i'/L'$, $k_i/k_H=k_i'/K_H'$ and $N_e=N_e'$ it easily follows that $l_iu\mu_o/k_i=l_i'u'\mu_o'P_c/k_i'P_c'$; hence, by comparing the right-hand side equations in (50) and (52) we find that

$$\int_{S_N}^{S_{N-1}^{+'}}F_N(S)\,\mathrm{d}S=\int_{S_N}^{S_{N-1}^{+}}F_N(S)\,\mathrm{d}S.$$

The integrand $F_N(S)$ does not change sign within the limits of integration, thus we conclude that

$$S_{N-1}^{+'}=S_{N-1}^{+}.$$

It follows that

$$S_{N-1}^{-'}=S_{N-1}^{-} \tag{53}$$

since corresponding saturation discontinuity functions are identical for the two media: $\Delta_{i,i-1}=\Delta_{i,i-1}'$, which is easily verified. Now repeat this argument for rock $N-1$, starting from (53). We finally obtain

$$S_0^{-'}=S_0^-=S_N$$

hence (49) is proved; in particular, $S'(x)$ is the periodic profile.

The result (49) implies that the two media have identical effective properties; more precisely, for each given f we have $(a_j)\,k_{rj}^{\text{eff}}=k_{rj}^{\text{eff}'}$ $(j=w,o)$, (b) $p_c^{\text{eff}}=p_c^{\text{eff}'}$ and (c) $S_{\text{eff}}=S_{\text{eff}'}$. To prove (a_j), recall that $k_{rj}^{\text{eff}}=u_j\mu_jL/k_H\Delta p_j$ (assume $u>0$

and $f \neq 0, 1$). Then, by our assumptions $M = M'$ and $N_e = N_e'$, it easily follows that (a_j) is true if and only if

$$\frac{\Delta p_j}{\Delta p_j'} = \frac{P_c}{P_c'}. \tag{54}$$

To check this we may take $j = w$. Recall that total pressure drop is given by (see (27), (29) and (30))

$$\Delta p_w = \sum_{i=1}^{N} (\Delta p_w)_i + \sum_{i \in A_w} (\Delta p_c)_i.$$

First compare the pressure drops $(\Delta p_w)_i$ over the ith rock in the two media. Starting from (13) in medium 2 we get

$$\begin{aligned}
(\Delta p_w)_i' &= \frac{f u' \mu_w'}{k_i'} \int_{x_{i-1}'}^{x_i'} \frac{1}{k_{rw}(S'(x))} \,\mathrm{d}x \\
&= f \int_{S_{i-1}'}^{S_i'} \frac{M'}{k_{rw}} F_i'(S) \,\mathrm{d}S \\
&= \frac{P_c'}{P_c} f \int_{S_{i-1}}^{S_i} \frac{M}{k_{rw}} F_i(S) \,\mathrm{d}S \\
&= \frac{P_c'}{P_c} (\Delta p_w)_i.
\end{aligned}$$

It remains to check that $(\Delta p_c)_i' = (P_c/P_c')(\Delta p_c)_i$ if $i \in A_w$. This follows easily from the assumption $p_c^{i'}(S) = (P_c'/P_c) p_c^i(S)$; thus (54) is proved. The claim (b) is proved similarly.

Finally we want to check the claim (c). By definition

$$S_{\text{eff}} = \frac{1}{\phi_A L} \sum \phi_i \int_i S(x) \,\mathrm{d}x, \tag{55}$$

where

$$\int_i S(x) \,\mathrm{d}x = \int_{x_{i-1}}^{x_i} S(x) \,\mathrm{d}x = \frac{k_i}{u \mu_o} \int_{S_{i-1}^+}^{S_i^-} S F_i(S) \,\mathrm{d}S,$$

or

$$\int_{S_{i-1}^+}^{S_i^-} S F_i(S) \,\mathrm{d}S = \frac{u \mu_o}{k_i} \int_{x_{i-1}}^{x_i} S(x) \,\mathrm{d}x. \tag{56}$$

Applying our result (49) we get in medium 2

$$\int_i S'(x)\,\mathrm{d}x = \frac{k'_i}{u'\mu'_o}\int_{S^{+\prime}_{i-1}}^{S^{-\prime}_i} SF'_i(S)\,\mathrm{d}S = \frac{k'_i P'_c}{u'\mu'_o P_c}\int_{S^+_{i-1}}^{S^-_i} SF_i(S)\,\mathrm{d}S.$$

Hence by (56)

$$\int_i S'(x)\,\mathrm{d}x = \frac{k'_i u\mu_o P'_c}{k_i u'\mu'_o P_c}\int_i S(x)\,\mathrm{d}x.$$

Therefore, since $k_i/k'_i = k_H/k'_H$, $\phi_i/\phi'_i = \phi_A/\phi'_A$, we get

$$S'_{\text{eff}} = \frac{1}{\phi'_A L'}\sum \phi'_i \int_i S'(x)\,\mathrm{d}x = \frac{k'_H u\mu_o P'_c}{k_H u'\mu'_o \phi_A L' P_c}\sum \phi_i \int_i S(x)\,\mathrm{d}x. \qquad (57)$$

Comparing (55) and (57) we find that $S'_{\text{eff}} = S_{\text{eff}}$ if and only if $N'_e = N_e$, thus (c) holds.

5.5. RELATION TO OTHER WORK

Capillary limit effective parameters have been studied by several authors; a number of different approaches have been applied: Volume averaging methods (Quintard and Whitaker [17–19]), stochastic methods (Shvidler ([21]), method of multiple scales combined with perturbation methods (where capillary equilibrium is apparently an implicit assumption) (Saez *et al.* [20], Amaziane *et al.* [2], Amaziane and Bourgeat [3], Bourgeat [4]), numerical methods (Smith [22]), percolation theory (Yortsos *et al.* [24]), self-consistent approximation (Ekrann *et al.* [12]). The paper [19] reports on several numerical experiments performed in order to identify the range of validity of the capillary limit condition in one dimension, analogous to our Section 6. Studies of the viscous limit effective parameters are more scarce (Smith [22], Dale [7]).

The main purpose of the present paper is to fill the gap between these two limiting cases, by constructing effective parameters for intermediate values $0 < u < \infty$ of the total velocity u, under the separation of scales condition. Trying to avoid scale constraints may lead to ill-defined effective parameters, see Quintard and Whitaker [9]. In their theory, the non-uniform saturation profiles generated when the capillary equilibrium and separation of scales conditions are removed, lead to effective relative permeabilities that are not well-behaved (pp. 460–467).

Using stochastic analysis and perturbation theory, Chang *et al.* [6] and Abdin *et al.* [1] study effective parameters of steady state flow in a randomly heterogeneous one-dimensional medium. Based on a specific choice of correlation function for absolute permeability, and an exponential relationship between relative permeability and capillary pressure, they derive first-order perturbation formulas for the

effective relative permeabilities. However, saturation does not enter explicitly in their set-up, therefore it is difficult to compare their results to ours.

The possibility of discontinuous capillary pressure at the interface between different rocks, and its influence on effective parameters (see Equations (18)–(23)), is not considered by any of the above authors. This problem ('the extended pressure condition') is studied in [9] by C. J. van Duijn *et al.*; their results are consistent with ours.

6. Applicability of Capillary Limit Effective Parameters

The methods detailed have been implemented into a software package, EFFECTIVE, facilitating convenient computation of two-phase effective parameters for one-dimensional heterogeneous media. This software has been used to compare capillary and viscous limit effective parameters with their finite velocity counterparts. In two-dimensional and three-dimensional models, the capillary limit assumption tremendously simplifies determination of effective parameters. In fact, analytical results are available only for this limit. Thus, the question of applicability of capillary limit effective parameters is of practical importance. It should be borne in mind, though, that the computations to be reported were carried out in one dimension, and thus do not tell the full story about two-dimensional and three-dimensional problems.

Computations were carried out for water wet and mixed wet media. Viscosities were always 1.0 cp and 2.0 cp for water and oil, respectively. In the water-wet media individual rocks were assumed to have identical relative permeabilities, and capillary pressures determined by the absolute permeability

$$p_c^i(S) = J(S)\frac{\gamma\sqrt{\phi_i}}{\sqrt{k_i}}. \tag{58}$$

Here, γ is surface tension, ϕ porosity, and $J(S)$ a Leverett J-function.

Results are presented versus an inverse macroscopic capillary number

$$\varepsilon = \frac{\gamma\sqrt{k_H\phi}}{L\mu_o u} \tag{59}$$

giving a measure of the ratio between capillary and viscous forces (Yortsos and Chang [23]; Chang and Yortsos [5]). Note that ε does not give a complete description; it does not react to the shape of the J-function, nor to variation of water viscosity or to sequencing of rocks. In the mixed wet media, we need to define a pseudo surface tension

$$\gamma = \frac{\sqrt{k_H}}{\sqrt{\phi}}\delta p_c, \tag{60}$$

where

$$\delta p_c = \frac{1}{N}\sum_{i=1}^{N}(p_c^i(S_{wc}^i) - p_c^i(1 - S_{or}^i)) \tag{61}$$

from which ε can be defined. Absolute permeability enters in a square root, because of the correlation with capillary pressure. In the experiments to be reported, ε is varied by varying L.

6.1. WATER-WET MEDIA

Two different heterogeneous media were constructed from 5 rocks of equal length, having absolute permeabilites $k_i = i$ D for $i = 1, \ldots, 4$ and $k_5 = 0.25$ D. Porosity is 0.25 for all rocks. Relative permeabilities are $k_{rw} = S^2$, $k_{ro} = (1 - S)^2$ for all rocks. To investigate the effect of the shape of the J-function, two formulas were used in the calculations:

$$J(S) = 1 - S,$$

$$J(S) = (1 - S)(2S^2 - 2S + 1).$$

Two different sequencings have been considered: Medium A has 2-5-1-3-4 (left to right), and medium B has 5-1-2-3-4. The interfacial tension is 20×10^{-3} N/m. Only medium B appeared to be sensitive to the shape of the Leverett J-function.

6.2. MIXED WET MEDIA

Two different media were used, each composed of 3 rocks of equal length. Rocks all have absolute permeability 1. Medium D and porosity 0.25. Capillary pressure curves for individual rocks are shown in Figure 7. For medium C, rock relative permeabilities were:

	Rock 1	Rock 2	Rock 3
k_{rw}	$0.2S^2$	S^2	$0.5S^2$
k_{ro}	$(1 - S)^2$	$0.2(1 - S)^2$	$0.5(1 - S)^2$

Medium D differed from medium C only by its relative permeability curves, which in this case were the same for all rocks, $k_{rw} = S^2$, $k_{ro} = (1 - S)^2$.

6.3. RESULTS

As examples of effective parameters, medium A (nonlinear Leverett J-function) effective relative permeabilities are shown for different capillary numbers in Figure 5.

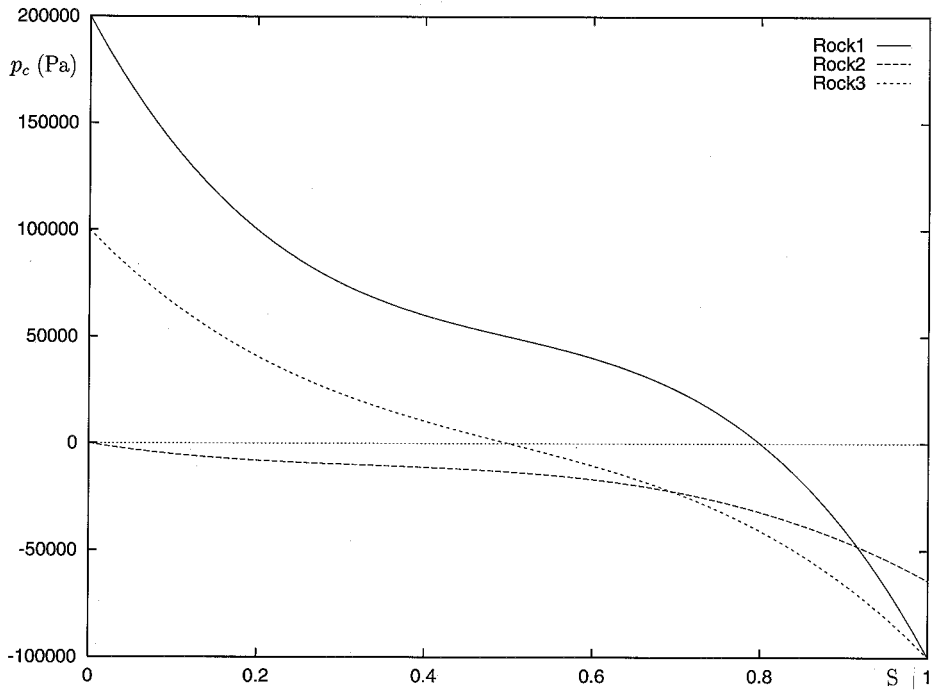

Figure 7. Rock 1–3 capillary pressures.

Results are otherwise presented in two ways: Table I is based on visual observations. An entry C.L. indicates that effective relative permeability curves practically coincide with their capillary limit counterparts. Similarly, V.L. indicates coincidence with viscous limit curves. No distinction is made in the table between the two different Leverett J-functions.

The same results are presented in Figures 8 and 9, showing $S_{wc}^{\text{eff}} - S_{wc}^{\text{cap}}$ (ΔS) and $k_{ro}^{\text{eff}}(S_{wc}^{\text{eff}}) - k_{ro}^{\text{cap}}(S_{wc}^{\text{cap}})$ (Δk_{ro}), respectively, both versus the capillary number, ε. In the figures, we have distinguished between positive ($+$) and negative ($-$) direction of flow. For medium B, we also distinguish between linear (l) and nonlinear (n).

The picture emerging is the same as that in the tables: For $\varepsilon \geqslant 100$, we are always practically at the capillary limit, while $\varepsilon \leqslant 0.1$ is close to the viscous limit. With the data given, and $u = 10$ cm/d, $\varepsilon = 100$ corresponds to $L \approx 0.1$ m for media A and B. Thus, only for very small scale heterogeneities can we guarantee applicability of capillary limit parameters in these low capillarity cases. Media C and D have capillary forces a factor of about 20 larger, and $\varepsilon = 100$ corresponds to $L \approx 2$ m. Even in these cases, therefore, applicability of capillary limit parameters can be guaranteed only for sub meter-scale heterogeneities, although this depends on the accuracy required.

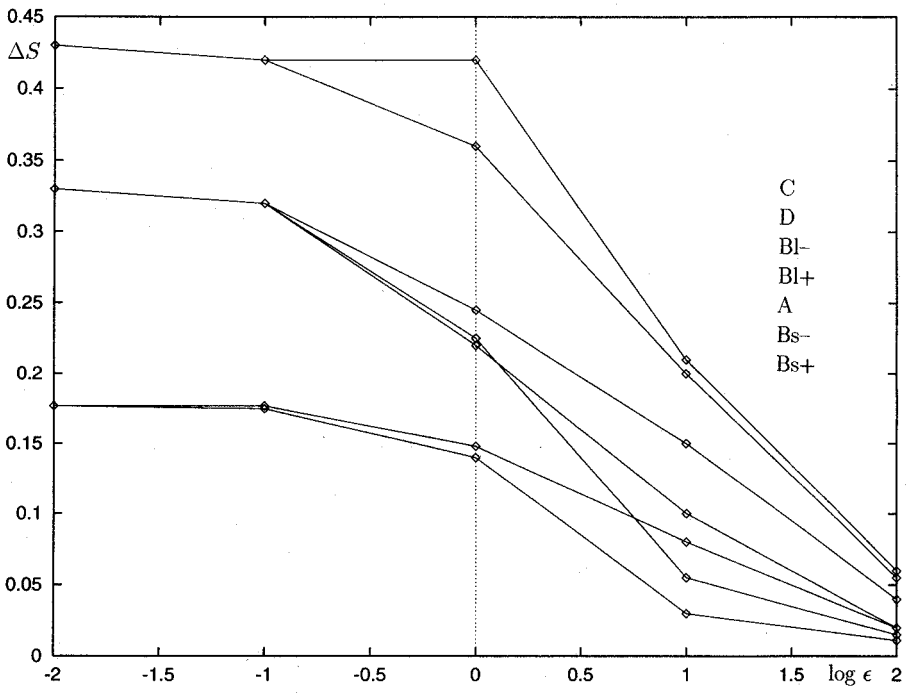

Figure 8. Difference in irreducible water saturation.

Table I. Rate dependence of effective relative permeabilities.

Medium	ε			
	0.1	1	10	100
A	V.L.	—	C.L.	C.L.
B	V.L.	—	—	C.L.
C	V.L.	—	—	C.L.
D	V.L.	—	—	C.L.

7. Numerical Displacement Experiments

7.1. INTRODUCTION

In practical situations, the conditions for validity of effective parameters discussed in Section 2 are never satisfied in a strict sense. Also, the steady-state approach taken may seem to be too restrictive. The question immediately arises, therefore, as to the applicability of our effective properties in real-life problems. In this section, we report some numerical experiments to address this question. Displacement of oil by water was considered, in one-dimensional reservoirs. For a given heterogeneous

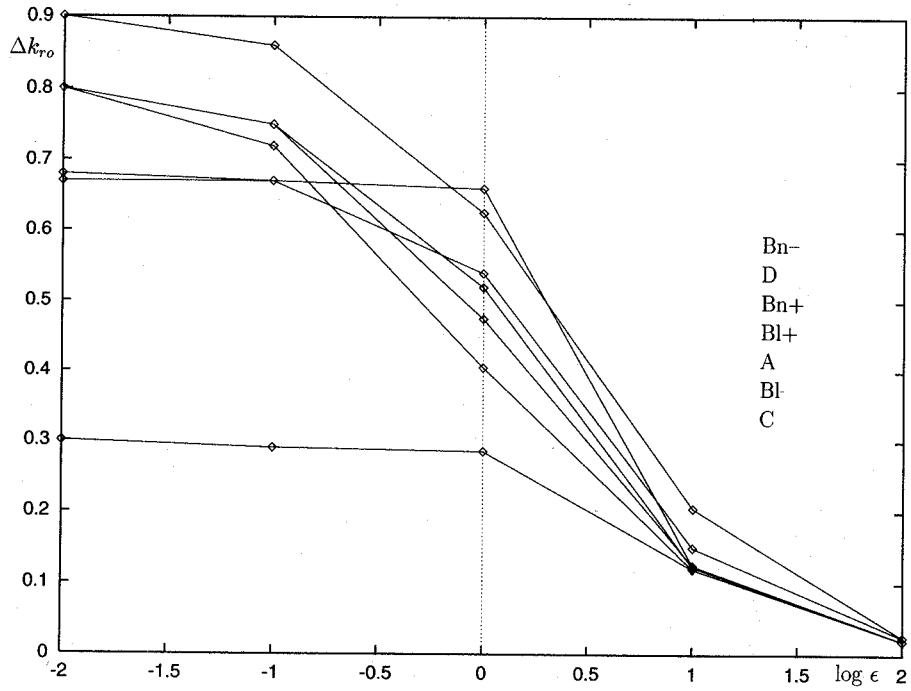

Figure 9. Difference in endpoint oil relative permeability.

reservoir, a detailed simulation of the process provided a 'true' solution. The same process (identical initial and boundary conditions) was then simulated in a homogeneous reservoir of the same total length, with rock properties equal to the effective properties of the original medium, computed as detailed previously. The discrepancy between these two solutions is then taken as a measure of applicability of the effective properties in the case in question.

7.2. EXPERIMENTAL SETUP

Heterogeneous media A and C were considered, see Section 6. In medium A, we used $J(S) = (1 - S)\,(2\,S^2 - 2\,S + 1)$. Individual rocks were taken to be 20 cm long in each case, and the reservoirs were each made up of 20 periods, providing for a total reservoir length of 20 and 12 m, respectively.

Reservoirs were initially 100 percent saturated with oil. We wanted water to be injected at a constant pressure, and production to take place at a given rate. The reservoir simulator used handles flow to wells somewhat unphysically ([10]), inasmuch as the well block *oil* pressure is used for both phases. This prevents imbibition at the inlet, and outlet end effects. A dummy block was added at the inlet, with a very large pore volume and large permeability, and with large fluid and rock compressibilities. Its capillary pressure is zero. Initially, the block is

Table II. Cases.

Case	Medium	u (cm/d)	μ_w (cp)	ε
A1	A	0.864	0.1	39
C1	C	0.864	0.1	$1.6\ 10^3$
C9	C	86.40	10	16

100 percent water saturated. This approximates the constant pressure boundary condition wanted, while allowing for countercurrent imbibition. At the outlet, an extra dummy gridblock was added, of the same size as the standard gridblocks (see below). Permeability is high, and capillary pressure zero, allowing for outlet end effects.

In the reservoirs, fluids (and rocks) were taken to be (almost) incompressible. Oil viscosity was always 2 cp. The three different cases considered are shown in Table II. In the table, ε was computed according to (59), with γ computed according to 61 if necessary. Note that water viscosity is not taken into account in these formulas. The experiments reported in Section 6 used $\mu_w = 1$ cp. In comparison, $\mu_w = 0.1$ cp and $\mu_w = 10$ cp should imply less and more influence by viscous forces, respectively, in particular at high water saturations. The low velocities for cases A1 and C1 was chosen not for realism, but to put our methods to a severe test.

Judging by the capillary numbers, we expect case C1 to be very close to the capillary limit. Also, case A1 would be expected to be capillary dominated, while case C9 is more intermediate.

Effective oil relative permeabilities are not defined at zero water saturation. Due to the way the simulations were carried out (100 percent oil initially), we augmented the curves produced by EFFECTIVE by feeding the simulator the correct (one-phase) effective oil relative permeability at $S = 0$.

In simulating displacement in these heterogeneous reservoirs, and their homogeneous counterparts, we have used a uniform grid with $\Delta x = 0.01$ m (except for the dummy inlet block). The main practical advantage offered by effective parameters, of course, is the possibility to handle small-scale heterogeneities accurately with coarse numerical grids. However, effective parameters are material properties, defined without any reference to numerical grids or to numerical simulation. We have chosen to focus on these fundamental aspects, and used the fine grid even for the homogeneous reservoirs to eliminate numerical effects as an issue.

7.3. RESULTS

Simulation results are presented in Figures 10–16. Each figure shows results from a heterogeneous reservoir (full line) and the corresponding homogeneous reservoir

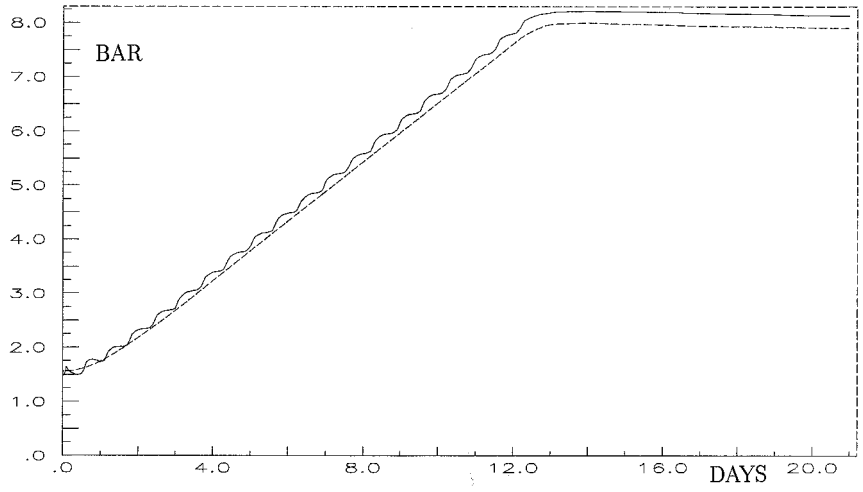

Figure 10. Pressure drop, case C9.

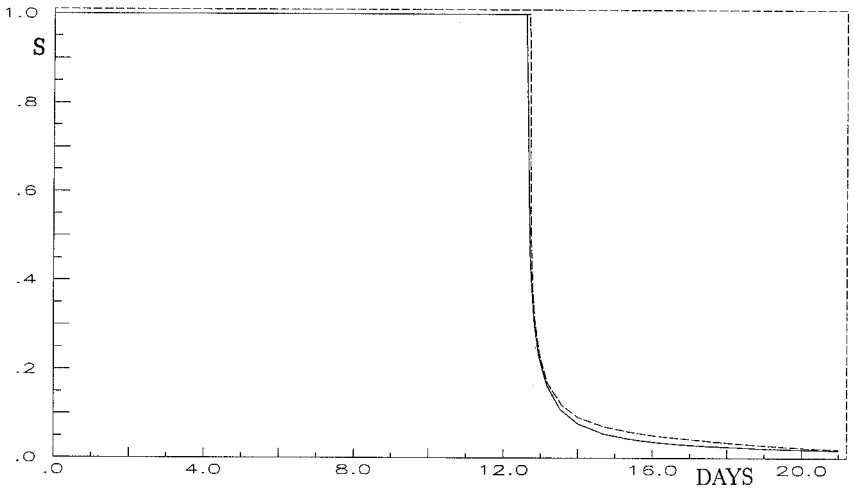

Figure 11. Producing oil fraction, case C9.

(dashed line). Results from case C1 are not presented, being quite similar to the C9 case.

Figures 10 and 13 show pressure drops vs. time. Pressure drops in heterogeneous reservoirs are measured from the inlet gridblock to the last gridblock in the last rock of the same type, and between the same gridblocks in the homogeneous reservoirs.

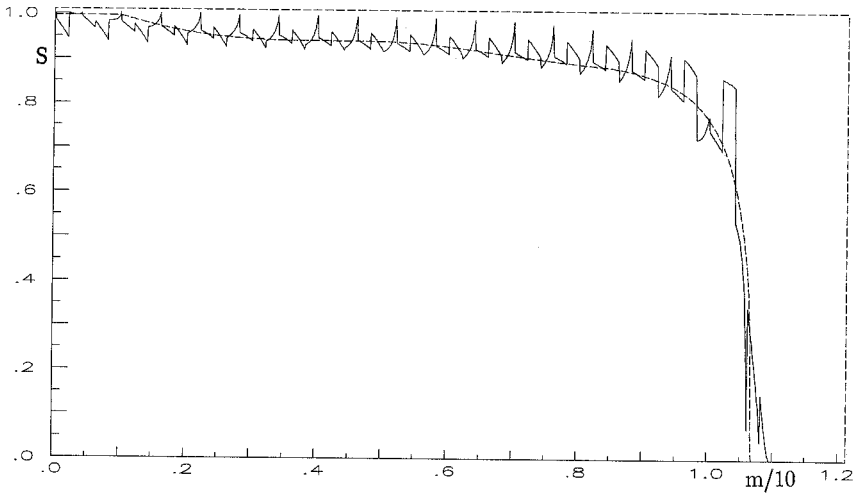

Figure 12. Saturation distribution after 0.6 PV case C9.

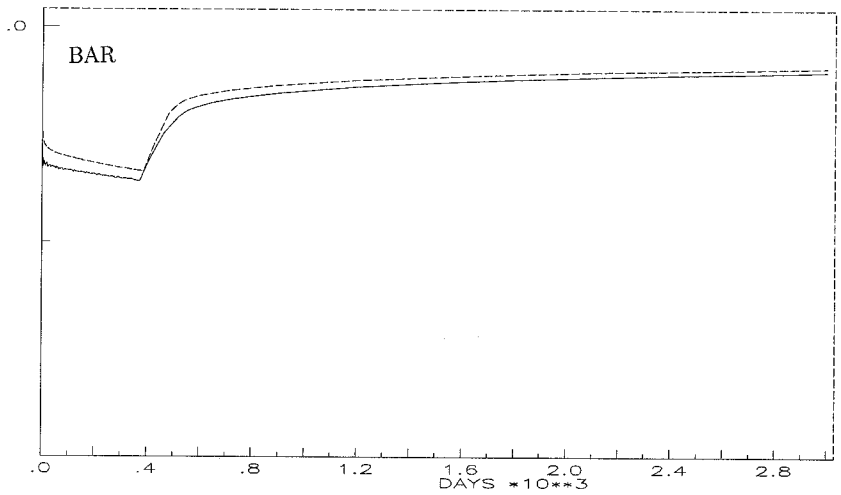

Figure 13. Pressure drop, case A1.

7.4. DISCUSSION

Results are quite satisfactory, in particular for case C9, where breakthrough is off by less than 2 percent, and final pressure drop by some 2.5 percent (Figures 11 and 10). Total production is slightly larger from the homogeneous reservoir, while backproduction (not shown) is larger (0.6 percent of original oil in place, vs. 0.2 percent) from the heterogeneous one. These slight discrepancies are presumably caused by end effects.

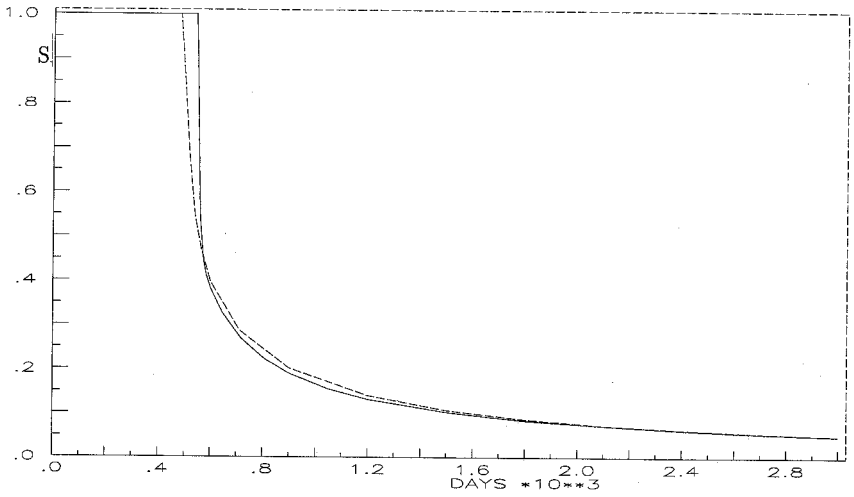

Figure 14. Producing oil fraction, case A1.

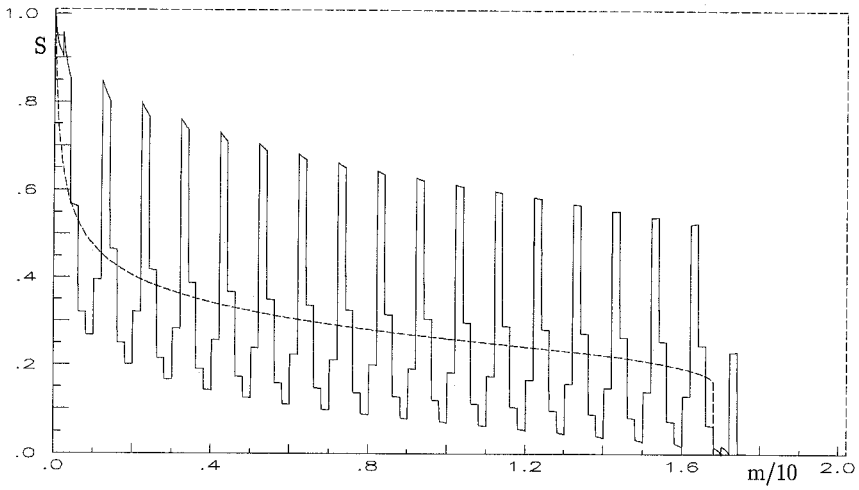

Figure 15. Saturation distribution after 0.13 PV, case A1.

Note from Figures 12 and 13 how the homogeneous reservoir averages the saturation distribution obtained in its heterogeneous counterpart. These figures also illustrate why the steady-state approach taken in developing the pseudos is not as limiting as it may appear: Behind the front, the average saturation is seen to be reasonably constant. Thus, the separation of scales condition is well satisfied, and the saturation distribution is close to what it would be in steady state, at the prevailing fractional flow.

In the front region separation of scales is clearly not satisfied. Even so, the front seems to be reasonably well approximated. Whether this is an artifact of our

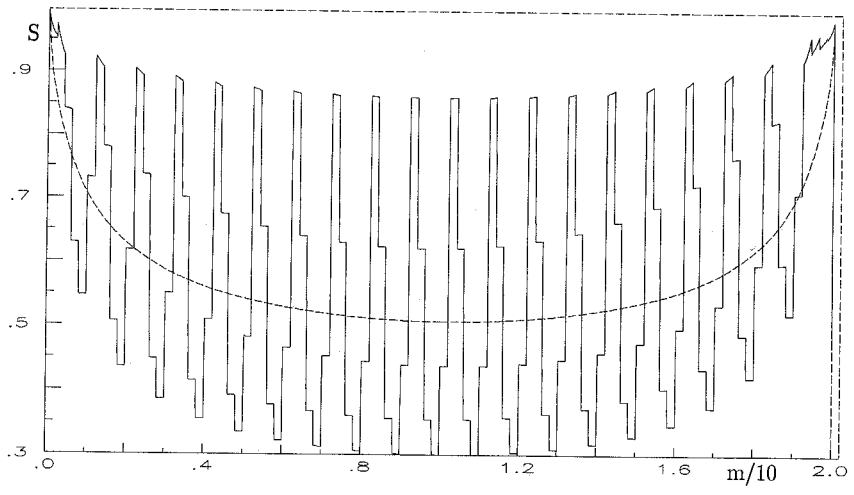

Figure 16. Saturation distribution after 1.3 PV, case A1.

particular examples has not been established. In any case, the front region would normally be short compared to the total reservoir length. Inaccurate treatment would therefore presumably have but a small effect on overall performance.

Case C1 (not shown) is heavily capillary dominated, as witnessed by $\varepsilon = 1.6\,10^3$. Capillary end effects are very important. Performance is almost as good as in the C9 case. Breakthrough is off by some 2.5 percent. Backproduction has doubled from the C9 case.

Case A1 is capillary dominated, and water wet, which resulted in large backproduction (about 25 percent of original oil in place). Countercurrent flow is not considered when computing effective properties, see Section 4, where $0 \leqslant f \leqslant 1$ is assumed. Also, spontaneous imbibition is an inherently transient process, for which our steady-state approach conceivably may be inappropriate. Finally, Figure 16 shows pronounced end effects, persisting for a significant part of the reservoir, causing the average saturation to be far from constant in these regions. Performance may still be considered acceptable, however. This is heartening, indicating that effective properties may be applicable in a wide range of practical situations.

8. Summary and Conclusions

We have constructed the effective relative permeability curves and the effective capillary pressure curve for a heterogeneous one-dimensional porous medium. The unit cell for the heterogeneities is composed of a finite number of homogeneous rocks in series. All rock parameters, including relative permeability curves and capillary pressure curves, are allowed to vary independently between different rocks.

The effective parameters are determined on the basis of the steady state saturation distribution in the medium, with periodic boundary conditions. Capillary equilibrium is not assumed, thus saturation distribution is allowed to vary within the averaging volume. Special care has to be taken with respect to pressure discontinuities at the interface between neighbouring rocks; this phenomenon may occur if neighbouring rocks have different capillary pressure endpoint values. In these cases, the common harmonic averaging procedure to calculate effective relative permeabilities has to be modified.

The effective parameters are generally rate dependent. By letting the rate tend to zero, keeping all other rock and fluid parameters fixed, we show that the well known effective properties for capillary equilibrium conditions result. As the rate tends to infinity, we obtain the effective properties for viscously dominated flow. The effective parameters as functions of the correlation length show the same convergence behaviour: As the correlation length increases from zero to infinity, corresponding effective parameters vary from the capillary limit to the viscous limit parameters.

By construction, our effective parameters are applicable when the spatial separation of scale conditions are satisfied, and the flow is sufficiently slowly varying. To study their applicability in dynamic displacement situations, we compare fine gridded simulations in heterogeneous media with simulations in their homogeneous, effective counterparts. Performance is quite satisfactory, even with strong fronts present, indicating that our effective properties may be applicable in a wide range of practical situations.

Acknowledgements

This work has partly been financed and performed as part of the Program for Research On Field Oriented Improved Recovery Technology (PROFIT), which is a joint Norwegian research program between Amoco Norway Oil Company, BP Norway Limited U.A, Conoco Norway Inc, Deminex (Norge) A/S, Elf Petroleum Norge A/S, Fina Exploration Norway u.a.s, Norsk Agip A/S, Norsk Hydro a.s, Norwegian Petroleum Directorate, Petrobras Norge A/S, Phillips Petroleum Company Norway, Saga Petroleum A.S and Statoil. The authors thank the PROFIT Board for permission to publish this paper.

The work was further supported in part by a grant from Norges Forskningsråd. The main parts of the paper was written during the first author's sabbatical leave 1993/1994 at the Department of Petroleum Engineering, Stanford University, California.

References

1. Abdin, A., et al.: 1995, Stochastic analysis of flow in porous media II: Comparison between perturbation and Monte-Carlo results, *Transport in Porous Media* **19**, 261–80.

2. Amaziane, B., Bourgeat, A. and Koebbe, J.: 1991, numerical simulation and homogenization of two-phase flow in heterogeneous porous media, *Transport in Porous Media* **6**, 519–47.
3. Amaziane, B. and Bourgeat, A.: 1988, Effective behavior of two-phase flow in heterogeneous reservoirs, in: M. F. Wheeler (ed.), *Numerical Simulation in Oil Recovery*, IMA Vol. Math. Appl. 11, Springer-Verlag, New York, pp. 1–22.
4. Bourgeat, A.: 1984, Nonlinear homogenization of two-phase flows in naturally fractured reservoirs with uniform fracture distribution, *Comput. Methods Appl. Mech. Engrg.* **47**, 205–16.
5. Chang, J. and Yortsos, Y. C.: 1992, Effect of capillary heterogeneity on Buckley–Leverett displacement, *Sphere*, May, 285–293.
6. Chang, C-M. et al.: 1995, Stochastic analysis of two-phase flow in porous media: I. Spectral/perturbation approach, *Transport in Porous Media* **19**, 233–259.
7. Dale, M.: 1991, Effective relative permeabilities for a one-dimensional heterogeneous reservoir, in L. W. Lake, H. B. Carroll jr. and T. C. Wesson (eds), *Reservoir Characterization II*, Academic Press, pp. 652–655.
8. Dale, M.: 1995, Preprint, Rogaland University Center.
9. van Duijn, C. J., Molenaar, J. and de Neef, M. J.: 1995, The effect of capillary forces on immiscible two-phase flow in heterogeneous porous media, *Transport in Porous Media* **21**, 71–93.
10. ECLIPSE 100 Reference Manual 92A, Appendices, Intera, 1992.
11. Ekrann, S. and Dale, M.: 1992, Averaging of relative permeability in heterogeneous reservoirs, in: P. R. King (ed.), *The Mathematics of Oil Recovery*, Clarendon Press, Oxford, pp. 173–199.
12. Ekrann, S., Dale, M., Langaas, K. and Mykkeltveit, J.: 1996, Capillary limit effective two-phase properties for three-dimensional media, SPE Paper 35493.
13. Ekrann, S.: 1992, Effective properties, in: S. M. Skjæveland and J. Kleppe (eds), *SPOR Monograph Recent Advances in Improved Oil Recovery Methods for North Sea Sandstones Reservoirs*, Norwegian Petroleum Directorate, Stavanger.
14. Hinderaker, L., Skjæveland, S. M. and Nystrand, B. V.: 1992, Key parameters for Norwegian Sandstone reservoirs, In: S. M. Skjæveland and J. Kleppe (eds), *SPOR Monograph Recent Advances in Improved Oil Recovery Methods for North Sea Sandstones Reservoirs*, Norwegian Petroleum Directorate, Stavanger.
15. Marle, M. G.: 1981, *Multiphase Flow in Porous Media*, Editions Technip.
16. Mykkeltveit, J.: 1993, A proof of the capillary limit algorithm in EFFECT, Preprint, Rogaland Research Institute.
17. Quintard, M. and Whitaker, S.: 1988, Two-phase flow in heterogeneous porous media: The method of large-scale averaging, *Transport in Porous Media* **3**, 357–413.
18. Quintard, M. and Whitaker, S.: 1990, Two-phase flow in heterogeneous porous media I: The influence of large spatial and temporal gradients, *Transport in Porous Media* **5**, 341–79.
19. Quintard, M. and Whitaker, S.: 1990, Two-phase flow in heterogeneous porous media II: Numerical experiments for flow perpendicular to a stratified system, *Transport in Porous Media* **5**, 429–72.
20. Saez, A. E., Otero, C. J. and Rusinek, I.: 1989, The effective homogeneous behavior of heterogeneous porous media, *Transport in Porous Media* **4**, 213–38.
21. Shvidler, M. I.: 1989, Average description of immiscible fluid transport in porous media with small-scale inhomogeneity, Translated from *Izvestiya Akad. Nauk SSSR, Mekh. Zhidkosti i Gaza* **6**, 92–99.
22. Smith, E. H.: 1991, The influence of correlation between capillary pressur and permeability on the average relative permeability of reservoirs containing small scale heterogeneity, in: L. W. Lake, H. B. Carroll jr. and T. C. Wesson (eds), *Reservoir Characterization II*, Academic Press, New York, pp. 52–76.
23. Yortsos, Y. C. and Chang, J.: 1990, Capillary effects in steady-state flow in heterogeneous cores, *Transport in Porous Media* **5**, 399–420.
24. Yortsos, Y. C., Satik, C., Bacri, J.-C. and Salin, D.: 1993, Large-scale percolation theory of drainage, *Transport in Porous Media* **10**, 171–195.